



## **Measurement of the $\Lambda_c^+$ and $D_s^+$ Lifetimes \***

**P. L. Frabetti**

*Dip. di Fisica dell'Università and INFN - Bologna*  
*I-40126 Bologna, Italy*

**C. W. Bogart, H. W. K. Cheung, P. Coteus, S. Culy, J. P. Cumalat, D. Kaplan**  
*University of Colorado*  
*Boulder, Colorado 80309*

**J. N. Butler, F. Davenport, I. Gaines, P. H. Garbincius, S. Gourlay, D. J. Harding, P. Kasper,**  
**A. Kreymer, P. Lebrun, H. Mendez**  
*Fermi National Accelerator Laboratory*  
*P. O. Box 500*  
*Batavia, Illinois 60510*

**S. Bianco, M. Enorini, F. L. Fabbri, A. Spallone, A. Zallo**  
*Laboratori Nazionale di Frascati dell'INFN*  
*I-00044 Frascati, Italy*

**R. Culbertson, M. Diesburg, G. Jaross, K. Lingel, P. D. Sheldon, J. R. Wilson, J. Wiss**  
*University of Illinois at Urbana-Champaign*  
*Urbana, Illinois 61801*

**G. Alimonti, G. Bellini, M. Di Corato, M. Giammarchi, P. Inzani, S. Malvezzi,**  
**P. F. Manfredi, D. Menasce, L. Moroni, D. Pedrini, L. Perasso, A. Sala, S. Sala,**  
**D. Torretta, M. Vittone**  
*Dip. di Fisica dell'Università and INFN - Milano*  
*I-20133 Milan, Italy*

**D. Buchholz, C. Castoldi, B. Gobbi, S. Park, R. Yoshida**  
*Northwestern University*  
*Evanston, Illinois 60208*

**J. M. Bishop, J. K. Busenitz, N. M. Cason, J. D. Cunningham, R. W. Gardner, C. J. Kennedy,**  
**E. J. Mannel, R. J. Mountain, D. L. Puseljic, R. C. Ruchti, W. D. Shephard, M. E. Znanabria**  
*University of Notre Dame*  
*Notre Dame, Indiana 46556*

**S. P. Ratti**  
*Dip. di Fisica dell'Università and INFN- Pavia*  
*I-27100 Pavia, Italy*

**A. Lopez**  
*University of Puerto Rico*  
*Mayaguez, Puerto Rico 00700*

**August 1990**

\* Submitted to Phys. Lett. B.



## Abstract

Measurements of the lifetimes of the  $\Lambda_c^+$  decaying into  $pK^-\pi^+$  and of the  $D_s^+$  decaying into  $\phi\pi^+$  are presented. The data were accumulated in the Fermilab Wide-Band photoproduction experiment E-687. The lifetimes of the  $\Lambda_c^+$  and the  $D_s^+$  are measured to be  $(0.20 \pm 0.03 \pm 0.03) \times 10^{-12}$  s and  $(0.50 \pm 0.06 \pm 0.03) \times 10^{-12}$  s respectively.

Precision measurements of the lifetimes of the  $\Lambda_c^+$  and the  $D_s^+$  have been difficult to obtain compared to those of the  $D^0$  and the  $D^+$  charmed mesons because of both their reduced production rates and the shorter lifetime of the charmed baryon. Lifetime measurements of both the  $\Lambda_c^+$  <sup>1,2,3,4</sup> and the  $D_s^+$  <sup>5,6,7,8</sup> have, however, improved significantly during the last two years. Accurate measurements of these lifetimes are important in understanding the contributions of various weak decay processes such as the spectator, W-annihilation, and W-exchange decay mechanisms as well as QCD hard gluon exchange effects. In this paper we present new measurements of the  $\Lambda_c^+$  and the  $D_s^+$  lifetimes using the Fermilab Wide-Band Photon Spectrometer.

The E687 spectrometer has large acceptance for both charged and neutral hadrons. In addition, it has electromagnetic and hadronic calorimetry as well as muon identification. In this analysis, charged particles are traced with 12 silicon microstrip planes and 19 multiwire proportional planes and are identified as pions, kaons, or protons by 3 multicell Cerenkov detectors. Details of the spectrometer are presented elsewhere.<sup>9</sup>

The photon beam, incident on a Be target, was derived from electrons of 350 GeV/c momentum with a  $\pm 13\%$  momentum spread. The electrons impinged on a 27% radiation length target creating the bremsstrahlung photon beam. The photon beam was tagged by detection of the recoil electron. The experimental trigger required that at least two charged tracks be present in the spectrometer (both of which had to be outside the pair production region) and that an energy deposit of at least 35 GeV occur in the hadron calorimeter. The average tagged photon energy for this data sample was 221 GeV. Some 60 million triggers were recorded on tape during the experiment.

Both the  $\Lambda_c^+ \rightarrow pK^-\pi^+$  and the  $D_s^+ \rightarrow \phi\pi^+ \rightarrow K^+K^-\pi^+$  samples were obtained with a candidate-driven vertex finder using the silicon microstrip data. (In this paper, charge conjugate states are included when decay modes of a specific charge are discussed.) The algorithm worked as follows. A secondary vertex was first formed from three selected daughter tracks which were found in both the microstrip system and the PWC system and which were linked between the systems. The tracks were required to have a  $\chi^2$  per degree of freedom of less than 3.0 for originating from a common vertex and to have particle identification consistent with the assumed decay

mode. Next a seed track was constructed from the momentum vectors of the candidate daughter tracks. Other tracks consistent with intersecting the seed track were used to form a primary vertex candidate which was required to be upstream of the secondary vertex. Finally, the distance  $L$  between the secondary and primary vertices was calculated and divided by  $\sigma_L$ , the error on that difference. Typical errors on this distance, when converted to proper time, were 0.04 ps for the  $\Lambda_c^+$  candidates and 0.07 ps for the  $D_s^+$  candidates. For the  $\Lambda_c^+$  and the  $D_s^+$  analyses reported here, the cut on the significance of the vertex separation was chosen to be  $L/\sigma_L > 3.0$ .

The procedure used <sup>10</sup> to obtain the lifetimes was to employ a maximum likelihood fit utilizing a likelihood function which simultaneously describes the proper time and the mass dependences of the signal(s) as well as the background. With the cut on the significance of the vertex separation described above, one then obtains the lifetime by maximizing the likelihood function  $\mathcal{L}$ , properly normalized on an event-by-event basis over the allowed ranges of  $m$  and  $t$ , of the form:

$$\mathcal{L} = \sum_{i=1}^N \log(S_i + B_i).$$

Here  $S_i$  is the term for the signal(s) and  $B_i$  is the background term. Variables for the likelihood function are the effective mass  $m_i$  and either the proper time  $t$ , or the reduced proper time  $t'_i = (L - 3.0\sigma_L)/\beta\gamma c$  for each event. Both of these proper time variables have been employed in the  $\Lambda_c^+$  analysis as well as the  $D_s^+$  analysis in order to test the sensitivity of the results to the fitting procedure.

The data sample used for the  $\Lambda_c^+$  analysis was obtained by employing a variety of cuts prior to making the vertex separation cut described above. Combinations of three tracks consistent with the hypothesis  $\Lambda_c^+ \rightarrow pK^-\pi^+$  were first selected as described below. All candidate tracks were required to be reconstructed in the main spectrometer tracking system and to be successfully linked to a reconstructed microstrip track. Tracks consistent with a muon hypothesis were rejected. The proton and pion candidates were required to have the same charge, and the kaon candidate was required to have the opposite charge. Čerenkov cuts were applied: the proton track was required to be identified as a proton or K/p ambiguous; the kaon was required to be identified as a kaon or K/p ambiguous; and the pion track could not be identified as electron, kaon, proton or K/p ambiguous. If both proton and kaon candidates were ambiguous, the combination was rejected.

Cuts were also made on the cosine of the angle between each daughter track and the  $\Lambda_c^+$  momentum vector. The cuts on the angle as evaluated in the  $\Lambda_c^+$  rest frame were:  $\cos\theta < 0.9$  for the pion;  $\cos\theta > -0.9$  for the kaon; and  $-0.9 < \cos\theta < 0.9$  for the proton. These cuts significantly improved the signal to noise ratio. Finally an

additional cut required each  $\Lambda_c^+$  candidate to have an energy greater than 70 GeV. This energy cut further reduced the background.

In Fig. 1 is shown the combined mass distribution for accepted  $pK^-\pi^+$  after all of the above cuts. The fit to a Gaussian signal plus a linear background shown on the figure yields a signal with  $90 \pm 19$  events at a mass of  $2283 \pm 4$  MeV/c<sup>2</sup>. Fits to individual particle and antiparticle plots yield  $50 \pm 12$  and  $51 \pm 17$  event signals respectively.

The  $D_s^+$  lifetime was determined using a sample of  $\phi\pi^+$  decays of the  $D_s^+$  with  $\phi \rightarrow K^+K^-$ . The mass distribution for  $K^+K^-$  combinations where both tracks are required to be Čerenkov consistent with the kaon hypothesis shows a clear  $\phi$  peak. A fit to this distribution yields about 100,000  $\phi$ 's with a mean mass of  $1019.54 \pm .02$  MeV/c<sup>2</sup> and  $\sigma = 6.1 \pm 0.1$  MeV/c<sup>2</sup>. All  $\phi$  candidates with  $K^+K^-$  masses of  $1020 \pm 10$  MeV/c<sup>2</sup> were selected for the  $D_s^+$  analysis. The  $K^+$  and  $K^-$  tracks from these  $\phi$  candidates were then combined with single tracks identified in the Čerenkov system as consistent with the pion hypothesis to form the initial three-track combinations for vertexing which then proceeded as described above.

For the decay  $D_s^+ \rightarrow \phi\pi^+$ , the distribution for the angle between the  $K^+$  and the  $\pi^+$ , when viewed in the  $\phi$  rest frame, is expected to be  $dN/d\cos\theta \propto (\cos\theta)^2$ . The forward/backward peaking in the  $\cos\theta$  distribution can be exploited to improve the signal-to-background ratio in the  $D_s^+$  analysis since our spectrometer has flat acceptance in  $\theta$ . For the  $D_s^+$  analysis, a cut of  $|\cos\theta| \geq .3$  was used. This cut retained 97% of the signal while removing about 30% of the background.

The  $\phi\pi^+$  mass distributions for various cuts on the significance  $L/\sigma_L$  of the vertex separation were studied. Fig. 2 shows four plots of  $\phi\pi^+$  mass with different cuts on  $L/\sigma_L$ . Two prominent peaks are present. The higher-mass peak corresponds to the  $D_s^+$  and the lower to the Cabibbo-suppressed decay of the  $D^+$ . It is quite evident that as  $L/\sigma_L$  is increased the  $D^+$  peak gets increasingly larger relative to the  $D_s^+$  peak due to the fact that the  $D^+$  is longer-lived than the  $D_s^+$ .

For the final sample used in the  $D_s^+$  lifetime determination, a cut of  $L/\sigma_L > 3.0$  was imposed. A fit to the corresponding mass distribution with a function consisting of two Gaussian signals and a linear background yielded the  $D_s^+$  mass,  $\sigma$ , and signal shown in Table I. The fitted  $D_s^+$  mass (as well as that of the  $D^+$ ) agrees with the accepted value <sup>11</sup> within one standard deviation and the width is consistent with our resolution.

Studies of the proper time dependence of the background were performed using two mass sideband regions above the mass region containing the  $D_s^+$  and  $D^+$  signals as well as two regions below these signals; single mass sideband regions above and below the mass of the  $\Lambda_c^+$  were used. Fits of various functions were made to the distributions

in proper time for the background regions. Single-exponential and Gaussian functions did not adequately describe any of the background proper time distributions. Good fits could however be obtained with double exponential functions. The parameters of the functions determined from these fits were consistent with being mass-independent. The form of the background function  $B_i$  used in the final fits was thus chosen to be:

$$B_i = g(m_i) (\exp(-t_i/\tau_{B_1}) + C \exp(-t_i/\tau_{B_2})).$$

where  $g(m_i)$  was taken to be a linear function of the mass for the  $D_s^+$  sample and a quadratic function of the mass for the  $\Lambda_c^+$  sample. In addition, the variable  $t_i$  was replaced by  $t'_i$  for the  $\Lambda_c^+$  sample.

Monte Carlo events with no charm component were generated in order to understand the origin of the background events. After applying the same cuts which were applied to the data, the Monte Carlo proper time distribution also could not be fitted with a single exponential or with a Gaussian but was well described by the sum of two exponentials.

The  $\Lambda_c^+$  lifetime was determined by a maximum-likelihood fit to  $m$  and to the reduced proper time  $t'$ . The values of  $t'$  range from 0.0 to a maximum determined on an event-by-event basis requiring that the  $\Lambda_c^+$  decay occur upstream of a trigger counter just in front of the first microstrip plane. A combined fit of signal and background was made for events with mass between 2.10 and 2.45 GeV/c<sup>2</sup>. The mass parameters were fixed at values resulting from the fit to the mass distribution alone. Thus the function

$$S_i = \frac{A}{\sigma\sqrt{2\pi}} \exp \frac{-(m_i - m)^2}{2\sigma^2} \frac{f(t'_i)}{\tau} \exp \left( \frac{-t'_i}{\tau} \right)$$

and the background function described above were used in the likelihood function  $\mathcal{L}$ . The linear function  $f(t'_i) = F + Gt'_i$  in  $S_i$ , with  $F$  and  $G$  determined from Monte Carlo studies, includes the effects of spectrometer acceptance and of secondary-particle absorption in the target as a function of  $t'$ .

The fitted  $\Lambda_c^+$  lifetime is  $0.20 \pm 0.03$  ps. The proper time distribution for the final event sample along with the fitted curve, integrated over the mass distribution, is shown in Fig. 3a. The fitted values used in the background parameterization were:  $\tau_{B_1} = 0.10$  ps,  $\tau_{B_2} = 1.75$  ps and  $C = 0.25$ .

A study was made using different  $L/\sigma_L$  cuts to look for systematic effects due to correlations; no such effects were found. As an additional check, the lifetime was also determined with a binned maximum likelihood fit using a sideband background subtraction procedure similar to that used by Anjos *et al.*<sup>2</sup>. This fit yielded a  $\Lambda_c^+$  lifetime which agreed with that obtained from our other method within one standard

deviation. Inclusion of the correction function  $f(t')$  consistently reduced the measured lifetime by 0.02 ps in both types of fits compared to fits without this factor.

The  $D_s^+$  lifetime was determined using a maximum-likelihood fit of a function similar to that used in the  $\Lambda_c^+$  analysis. However, the likelihood function  $\mathcal{L}$  differed from that for the  $\Lambda_c^+$  in several ways. The proper time  $t$  was used as the fit variable rather than  $t'$ . Furthermore, the signal function  $S_i$  contained two terms, the first for the  $D_s^+$  decay and the second for the Cabibbo-suppressed decay of the  $D^+$ :

$$S_i = \frac{N_1}{\sigma_1 \sqrt{2\pi}} \exp \left( -\frac{(m_i - m_1)^2}{2\sigma_1^2} \right) \frac{f(t_i)}{\tau_1} \exp \left( -\frac{t_i}{\tau_1} \right) \\ + \frac{N_2}{\sigma_2 \sqrt{2\pi}} \exp \left( -\frac{(m_i - m_2)^2}{2\sigma_2^2} \right) \frac{f(t_i)}{\tau_2} \exp \left( -\frac{t_i}{\tau_2} \right).$$

The function  $f(t)$  is a correction function including the effects of acceptance as a function of proper time and of secondary particle absorption in the target. This function was determined on the basis of Monte Carlo studies and was parameterized as a second order polynomial in  $t$ .

The fit functions  $S_i$  and  $B_i$  were normalized over mass and proper time. For mass, they were normalized over the total mass range from 1.7 to 2.1 GeV/c<sup>2</sup>, while for proper time  $t$  they were normalized on an event-by-event basis over the range  $t_{min}$  to  $t_{max}$ . The value of  $t_{min}$  was  $3\sigma_{L_i}/(\beta\gamma c)$ , while  $t_{max}$  was determined by the requirement that the decay occur upstream of a trigger counter just upstream of the first microstrip plane. For the  $D_s^+$  lifetime fit, all variables, including the mass and the background parameters were varied simultaneously.

Fig. 3b shows the fit to the proper time  $t$  in the  $D_s^+$  mass region. The fit yielded a value of  $0.50 \pm 0.06$  ps for the  $D_s^+$  lifetime. The fitted lifetime for the Cabibbo-suppressed  $D^+$  was  $0.90 \pm 0.13$  ps. The fitted values for the background parameters were:  $\tau_{B_1} = 0.11 \pm 0.01$  ps,  $\tau_{B_2} = 0.53 \pm 0.07$  ps and  $C = 0.14 \pm 0.03$ .

Systematic effects were studied by doing fits for various values of the vertex separation parameter  $L/\sigma_L$ . We also varied the mass range over which the fit was done and varied other cuts used in the analysis over wide ranges. The resulting lifetime determinations did not vary by more than 0.03 ps. In addition, a fit was done without the acceptance correction factor  $f(t)$  to study the magnitude of the acceptance correction. In this case, the resulting values were  $0.53 \pm 0.07$  ps for the  $D_s^+$  lifetime and  $1.09 \pm 0.19$  ps for the  $D^+$  lifetime.

The final results from the  $D_s^+$  fit and that of the  $\Lambda_c^+$  fit are summarized in Table I. Also shown in the table are the previous world averages for these lifetimes. Our results are compared with other high statistics lifetime measurements in Table II. We note that our results will tend to raise the previous world average lifetimes of both the

$D_s^+$  and the  $\Lambda_c^+$ . Furthermore, as can be seen from Table II, the other high statistics experiments give results higher than the previous world averages.

We wish to acknowledge the assistance of the staffs of Fermilab, INFN of Italy and the physics departments of the University of Colorado, the University of Illinois, Northwestern University, and the University of Notre Dame. This research was supported in part by the National Science Foundation, the U.S. Department of Energy, the Italian Istituto Nazionale di Fisica Nucleare and Ministero della Universita' e della Ricerca Scientifica.

TABLE I. Results of the fits.

	$\Lambda_c^+$	$D_s^+$
Mass( $GeV/c^2$ )	$2.283 \pm 0.004$	$1.967 \pm 0.002$
Width( $GeV/c^2$ )	$0.019 \pm 0.004$	$0.011 \pm 0.003$
Signal(events)	$90 \pm 19$	$104 \pm 15$
Measured Lifetime(ps)	$0.20 \pm 0.03 \pm 0.03$	$0.50 \pm 0.06 \pm 0.03$
World Average(ps) <sup>a</sup>	$0.179^{+0.023}_{-0.017}$	$0.436^{+0.038}_{-0.032}$

<sup>a</sup>See Ref. 11.

TABLE II. Comparison of our results with other high statistics experiments.

	$\Lambda_c^+$ lifetime (ps)	$D_s^+$ lifetime (ps)
E691	$0.22 \pm 0.03 \pm 0.02^a$	$0.47 \pm 0.04 \pm 0.02^b$
NA32	$0.196^{+0.023}_{-0.020} \pm 0.03^c$	
E687 (This experiment)	$0.20 \pm 0.03 \pm 0.03$	$0.50 \pm 0.06 \pm 0.03$

<sup>a</sup>See Ref. 2.<sup>b</sup>See Ref. 8.<sup>c</sup>See Ref. 3.



\*Present address: Vector Research Company, 6903 Rockledge Drive, Bethesda, MD 20817, USA.

†Present address: IBM T.J. Watson Laboratories, Yorktown Heights, NY 10598, USA.

‡Present address: University of Oklahoma, Norman, OK 73019, USA.

§Present address: University of North Carolina-Asheville, Asheville, NC 28804, USA.

\*\*Present address: Cinvestav-IPN, A.P. 14-740, 07000 Mexico DF, Mexico.

††Present address: Fermilab, Batavia, IL 60510, USA.

‡‡Present address: Dipartimento di Elettronica, Università di Pavia, Pavia, Italy.

§§Present address: INFN - Pavia, I-27100 Pavia, Italy.

\*\*\*Present address: NIKHEF-H, 1009 DB, Amsterdam, The Netherlands.

†††Present address: University of Alabama, Tuscaloosa, AL 35487, USA.

<sup>1</sup>M. Aguilar-Benitez *et al.*, Phys. Lett. **189B**, 254 (1987).

<sup>2</sup>J.C. Anjos *et al.*, Phys. Rev. Lett. **60**, 1379 (1988).

<sup>3</sup>S. Barlag *et al.*, Phys. Lett. **218B**, 374 (1989).

<sup>4</sup>M.P. Alvarez *et al.*, CERN-EP/90-66, (1990).

<sup>5</sup>H. Becker *et al.*, Phys. Lett. **184B**, 277 (1987).

<sup>6</sup>S.E. Csorna *et al.*, Phys. Lett. **191B**, 318 (1987).

<sup>7</sup>H. Albrecht *et al.*, Phys. Lett. **210B**, 267 (1988).

<sup>8</sup>J.R. Raab *et al.*, Phys. Rev. **D37**, 2391 (1988).

<sup>9</sup>P.L. Frabetti *et al.*, "Description and Performance of the Fermilab E687 Spectrometer", to be submitted to Nuclear Instruments and Methods.

<sup>10</sup>L. Lyons and D.H. Saxon, Rep. Prog. Phys. **52**, 1015 (1989).

<sup>11</sup>B.P. Yost *et al.* (Particle Data Book), Phys. Lett. **B204**, 1 (1988).

## Figure Captions

FIG. 1. Effective mass distribution for  $pK^-\pi^+$  + c.c. combinations after all cuts. The curve is a fit using a Gaussian signal and a quadratic background.

FIG. 2. Effective mass distribution for  $\phi\pi$  combinations with varying cuts on the vertex separation significance parameter  $L/\sigma_L$ : (a)  $L/\sigma_L > 2.0$ ; (b)  $L/\sigma_L > 3.0$ ; (c)  $L/\sigma_L > 4.0$ ; and (d)  $L/\sigma_L > 5.0$ . The curves are fits using Gaussian signals and linear backgrounds.

FIG. 3. Proper time distributions for the  $\Lambda_c^+$  and the  $D_s^+$  signal regions. (a) The  $\Lambda_c^+$  region for which  $t' = t - t_{min}$  is plotted. (b) The  $D_s^+$  region for which  $t$  is plotted showing the effect of the  $t_{min}$  cut. The fitted curves are described in the text.

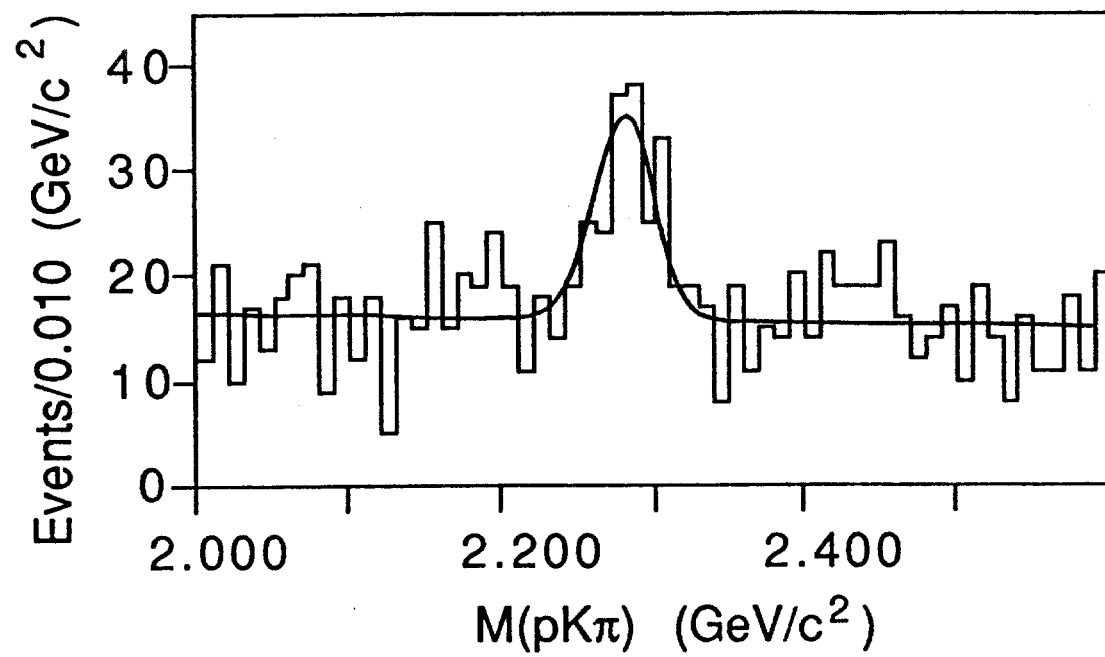


Figure 1

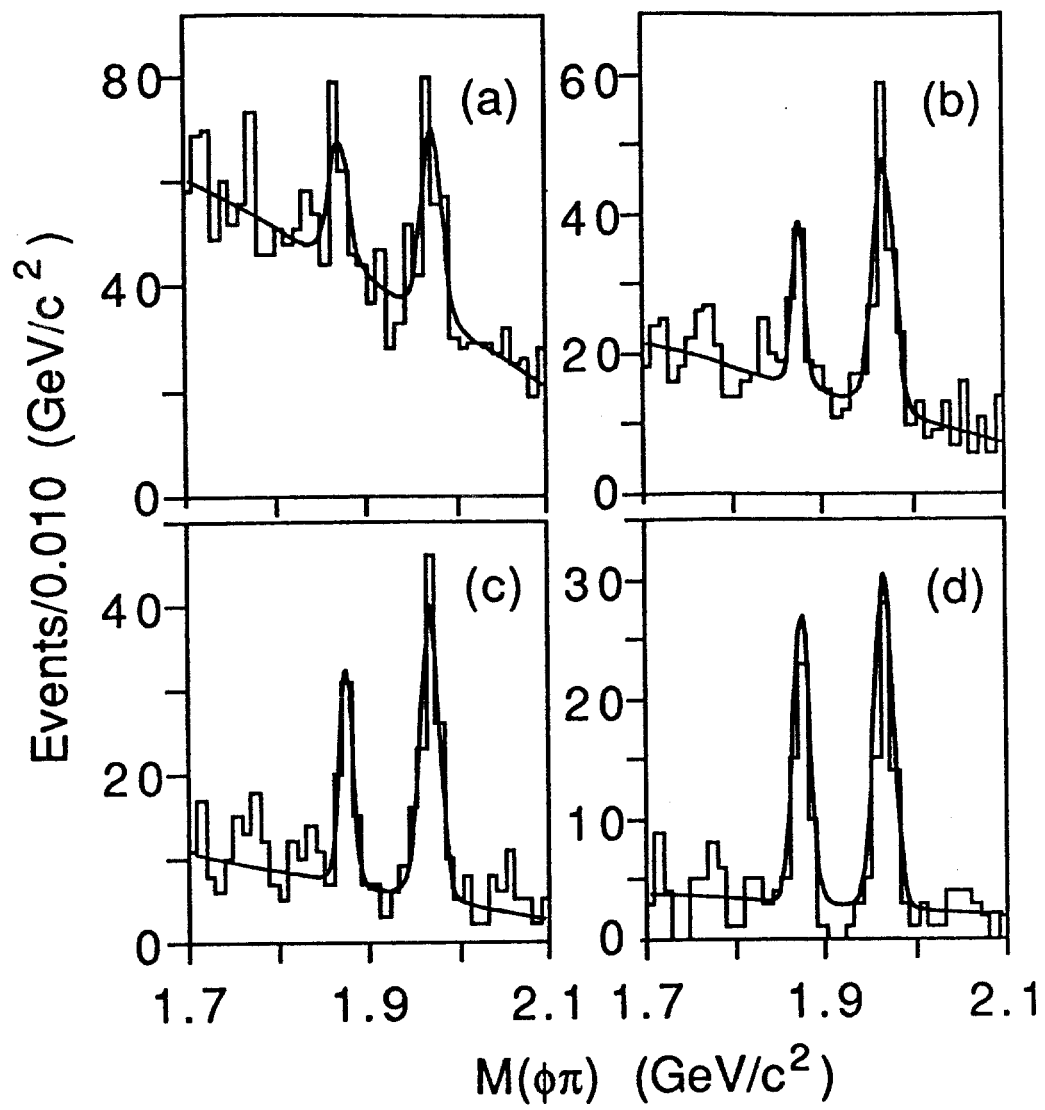


Figure 2

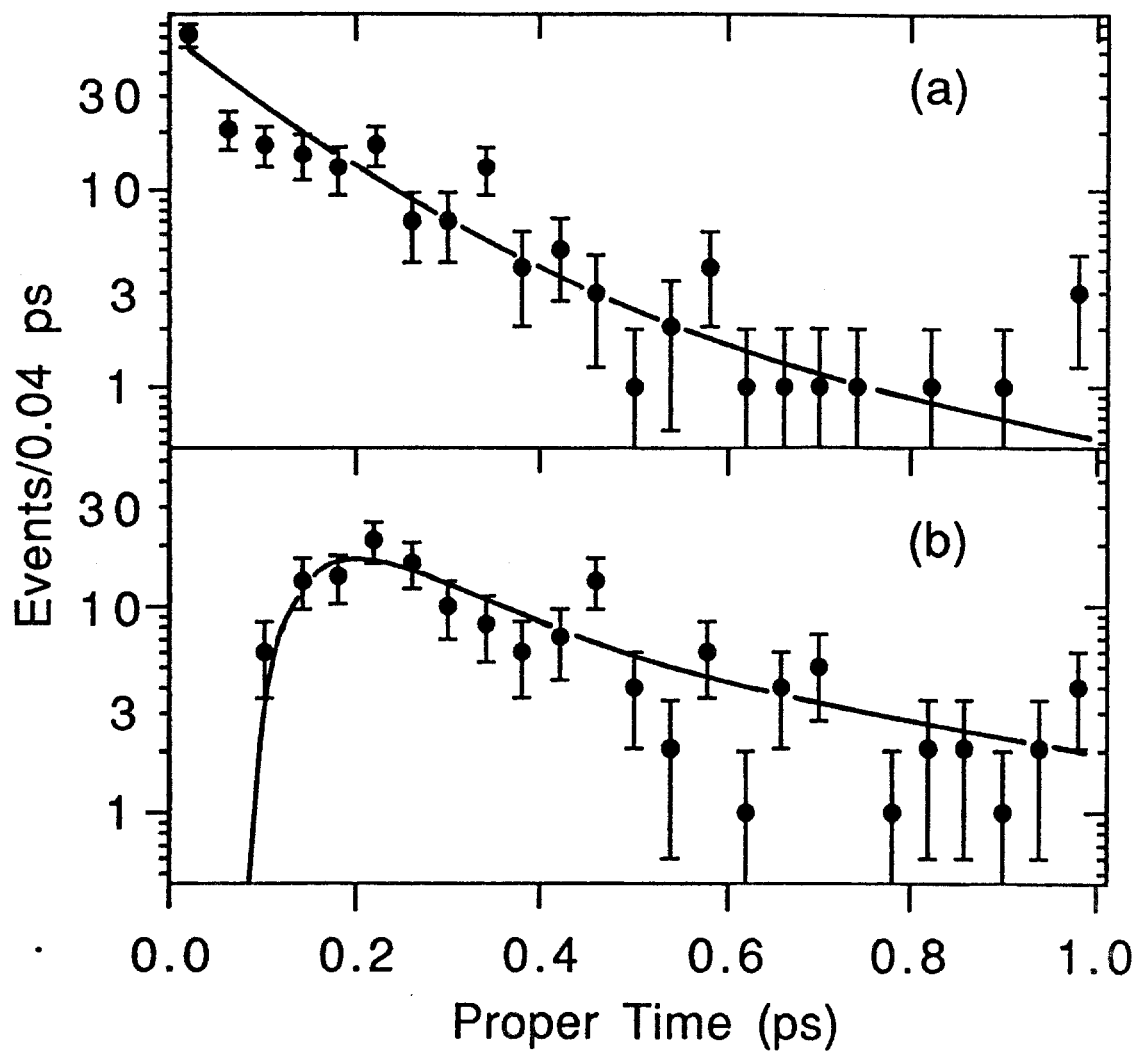


Figure 3